ISSN 1063-7826, Semiconductors, 2020, Vol. 54, No. 6, pp. 687–690. © Pleiades Publishing, Ltd., 2020.
Russian Text © The Author(s), 2020, published in Fizika i Tekhnika Poluprovodnikov, 2020, Vol. 54, No. 6, pp. 580–584.

Silicon Light-Emitting Diodes with Luminescence from (113) Defects

A. E. Kalyadin[a], K. F. Shtel'makh[a], P. N. Aruev[a], V. V. Zabrodskii[a], K. V. Karabeshkin[a], E. I. Shek[a], and N. A. Sobolev[a,]*

[a] *Ioffe Institute, St. Petersburg, 194021 Russia*

**e-mail: nick@sobolev.ioffe.rssi.ru*

Received February 10, 2020; revised February 17, 2020; accepted February 17, 2020

Abstract—Silicon light-emitting diodes with luminescence associated with (113) defects are fabricated by the implantation of 350-keV oxygen ions at a dose of 3.7×10^{14} cm^{-2} and subsequent annealing at 700°C for 1 h in a chlorine-containing atmosphere. The electroluminescence is studied in wide temperature and excitation-power ranges. The line associated with the (113) defects is dominant in all the spectra. The temperature dependence of the line intensity depends on the excitation power at low temperatures: an increase in the intensity with an activation energy of 25 meV is observed at low current densities and no rise in the intensity is observed with increasing current density. At higher temperatures, an intensity with an activation energy of 59 meV is quenched irrespective of the current density. With increasing temperature, the peak of the line of the (113) defect shifts by the same energy as the energy-gap width, whereas the half width of the line grows linearly.

Keywords: (113) defects, silicon, light-emitting diodes, electroluminescence

DOI: 10.1134/S1063782620060081

1. INTRODUCTION

The development of silicon optoelectronics requires that infrared (IR) light-emitting diodes (LEDs) for different wavelengths should be created. LEDs with luminescence from rare-earth ions Er^{3+} [1, 2] and with so-called dislocation-related luminescence associated with extended defects [3, 4] have already been fabricated for the wavelength range 1.5–1.7 μm, which corresponds to the second transparency range of quartz fibers. These LEDs are characterized by a high intensity of electroluminescence (EL) at room temperature. No LEDs have been developed so far for the wavelength range 1.3–1.4 μm, which corresponds to the first transparency window. Recently, attempts have been made in the development of light-emitting structures to use, as luminescence centers, those with which a line with a wavelength of ~1.37 μm is associated. This line is observed in a number of single-crystal silicon samples containing so-called (113) defects [5, 6]. In the initial stage of studies, the point of view that extended (113) defects are aggregations of intrinsic interstitial atoms with a structure different from that of dislocation dipoles and loops dominated [5]. Later, it was shown that vacancies are also involved in the formation of (113) defects [6]. The assumption that the emission line at a wavelength of 1.37 μm is associated with (113) defects formed during the double-stage prolonged annealing of Czochralski-grown silicon was made in [7]. Studies of samples implanted with Si^+ ions and then annealed in an inert atmosphere [8–10] or those implanted with O^+ ions and then annealed in a chlorine-containing atmosphere [11–13] by methods of high-resolution electron microscopy and photoluminescence confirmed that the line at 1.37 μm belongs to the (113) defect. It was also shown that photoluminescence is also observed above the temperature of liquid nitrogen (>77 K) [7, 9, 13]. This conclusion entailed studies aimed at creating LEDs with luminescence from (113) defects. To our knowledge, however, there is no information of this kind in publications. In the present study, we examine the dependence of the main parameters of the EL line associated with the (113) defect (intensity, peak position of the line and its half width) on the measurement temperature and current density in LED samples based on silicon implanted with oxygen ions.

2. EXPERIMENTAL

Boron was diffused from the gas phase into initial *n*-type Czochralski-grown silicon with resistivity of 4.5 Ω cm to form a p^+–n junction [4]. The surface concentration of boron and the depth of the p^+–n junction were ~10^{20} cm^{-3} and ~50 nm, respectively. Oxygen ions with an energy of 350 keV were implanted with a non-amorphizing dose of 3.7×10^{14} cm^{-2} on the side of the p^+-type layer. Implantation was performed at room temperature at an angle of 7° to avoid the channeling effect. The majority of oxygen ions were situated substantially deeper than the p^+–n junction

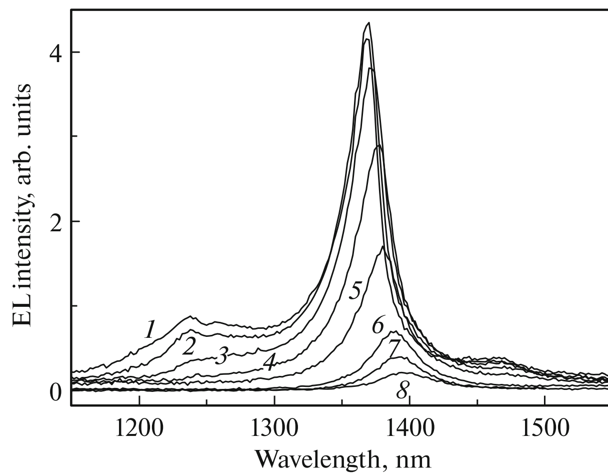

Fig. 1. EL spectra of LED structures at a current density of 4.61 A/cm^2 and various measurement temperatures T: (*1*) 30, (*2*) 50, (*3*) 70, (*4*) 90, (*5*) 110, (*6*) 130, (*7*) 150, (*8*) 170 K.

because the projected range of oxygen ions, calculated with SRIM software [14], was 790 nm. Subsequent annealing, during which defects introduced in the course of implantation were annealed out and luminescence centers were formed, was performed at a temperature of 700°C for 1 h in a chlorine-containing atmosphere, which had the form of a flow of oxygen saturated with a carbon-tetrachloride vapor with a molar concentration of 1%. As demonstrated by studies with the use of transmission electron microscopy and photoluminescence, (113) structural defects and related luminescence centers with a wavelength of 1.37 μm were dominant in light-emitting structures of this kind [13]. Ohmic contacts were formed by the vacuum evaporation of aluminum and its burning-in at a temperature of 420°C. Etching of the lateral surface of the samples with a mixture of hydrofluoric and nitric acids completed the fabrication of diode p^+–n mesa structures. The area of the structures was 3.7 mm^2. The EL spectra were measured with a resolution of 5 nm on an automated spectrometer based on an MDR-23 monochromator and an uncooled InGaAs photodiode. The sample was placed in a cryostat that provided measurement temperatures in the range of 4.2–300 K with an accuracy of ±0.2 K. The EL was excited with rectangular current pulses with a width of 15 ms, an amplitude of up to 160 mA, and a repetition frequency of 32 Hz. The emission was collected from the lateral surface of the diode structures. The parameters of the EL line associated with (113) defects were determined via its approximation with Gaussian curves.

3. EXPERIMENTAL RESULTS AND DISCUSSION

The EL spectra of the diode structures under study measured at temperatures of T = 30–170 K and a current density of 4.61 A/cm^2 are presented in Fig. 1 for wavelengths in the range 1150–1550 nm. The line dominant in the spectra is associated with (113) defects [13]. At a fixed measurement temperature, the peak position of this line is independent of the current density, and its amplitude steadily grows with increasing current. The half width of the line remains unchanged as the current increases. A characteristic feature of the line associated with (113) defects is that it has an asymmetric tail on the side of smaller wavelengths [8, 12]. The spectrum also shows two lines at wavelengths of ~1230 and ~1470 nm. Their intensity at low temperatures is substantially lower than that of the (113) defect line. These lines disappear as the temperature increases to more than 70 K and, therefore, are not considered here.

The experimental values of the peak positions of the line of the EL associated with (113) defects are shown as a function of temperature at current densities in the range from 0.58–4.61 A/cm^2 in Fig. 2. As the temperature increases, the luminescence line is shifted to longer wavelengths. The temperature dependence of the band-gap width of silicon (in meV) is described by the formula [15]

$$E_g(T) = 1169 - 0.49T^2/(T + 655), \tag{1}$$

where T is the temperature in K. Approximations of the dependences in Fig. 2 for the whole set of current densities (solid curve) demonstrated that the experimental temperature dependence of the peak position of the line of EL from (113) defects (E_{113}) is sufficiently well described by the dependence

$$E_{113}(T) = 907 - 0.49T^2/(T + 655) = E_g(T) - \Delta E, \tag{2}$$

where ΔE is temperature independent. The value of ΔE, found from our measurements, is (262 ± 1) meV. The error in determining ΔE is smaller than the instrumental measurement error. Formula (2) shows the energy position of (113) defects shifts in parallel with the decrease in the band-gap width of silicon. The experimentally determined temperature dependence of the peak positions of the EL line associated with (113) defects coincides with the similar dependence of the photoluminescence (PL) line associated with these defects [13]. It is noteworthy that the energy positions of the dislocation-luminescence lines $D1$ and $D2$ (associated with other related structural defects) decrease synchronously with the band-gap width of silicon with increasing temperature [3, 16–18].

It can be seen in Fig. 1 that the intensity of the EL line of (113) defects changes only slightly as the measurement temperature increases to ~70 K and decreases rather rapidly as the temperature grows further, being recorded up to 170 K. Figure 3 shows

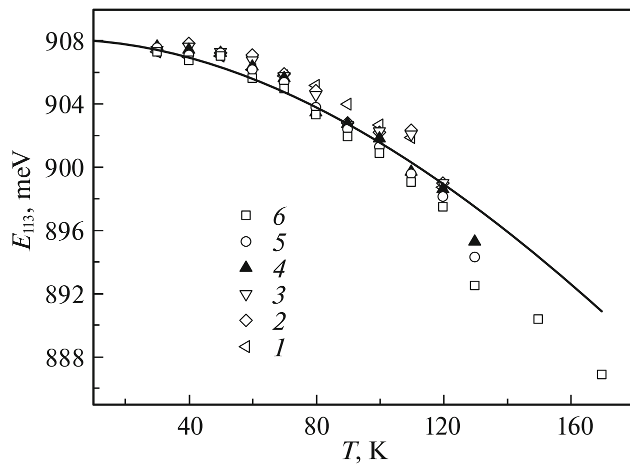

Fig. 2. Temperature dependences of the peak position of the EL line associated with (113) defects at different current densities: (*1*) 0.58, (*2*) 0.86, (*3*) 1.73, (*4*) 2.59, (*5*) 3.46, (*6*) 4.61 A/cm^2. The solid line represents the approximation with formula (2).

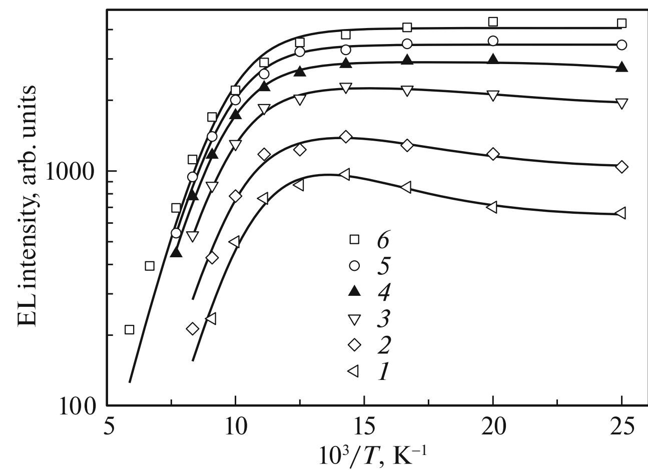

Fig. 3. Dependence of the intensity of the EL line associated with (113) defects on inverse temperature at different current densities: (*1*) 0.58, (*2*) 0.86, (*3*) 1.73, (*4*) 2.59, (*5*) 3.46, (*6*) 4.61 A/cm^2. The solid lines are approximating curves plotted in accordance with (3).

experimental values (points) of the integrated intensity (I) of lines of luminescence from the (113) defect on the inverse temperature for current densities in the range of 0.58–4.61 A/cm^2. The dependences obtained are well described by the formula [19]

$$I(T) = I(0)\{1 + C/[1 + B\exp(-E/kT)T^n]\}^{-1} \times [1 + D\exp(-W/kT)T^n]^{-1}. \quad (3)$$

Here, W and E are the activation energies of luminescence buildup and quenching, respectively; A, B, and C are the model parameters dependent on the current density; k is the Boltzmann constant, and $n = 1.5$. The approximating curves are also shown in Fig. 3 (solid lines). The activation energies of luminescence buildup and quenching are (25 ± 5) and (59 ± 8) meV, respectively. The lower three curves are the well-known dependences, in which, as the temperature increases, first a buildup of the luminescence intensity is observed and then its decay [19]. The buildup of the luminescence intensity is accounted for by the fact that excitons are captured at shallow centers at low temperatures, are released as the temperature increases, diffuse, and then are captured and radiatively recombine at a luminescence center. In our case, the relative luminescence-intensity buildup of the line associated with the (113) defect decreases as the current density increases from 0.58 to 1.73 A/cm^2 and is not observed at higher current densities. This effect can be explained as follows. At a low current density, the concentrations of shallow capture centers and excitons introduced by passing a current are comparable. Therefore, a substantial luminescence-intensity buildup occurs upon a thermal release of excitons. As the concentration of excitons being introduced starts to exceed that of capture centers and, accordingly, the concentration of thermally released excitons, the effect of the luminescence-intensity buildup becomes weaker, and, beginning at certain current densities, no buildup portion is observed. The quenching of the EL intensity is due to deactivation of the excited state of a (113) center and/or to the appearance of nonradiative-recombination centers. As a rule, this process has the form of multiphonon nonradiative recombination. The values of the EL-buildup- and quenching-activation energies well coincide with the values of the corresponding energies for the case of PL. This means that, when mesa LEDs are fabricated (ohmic contacts and edge contour are formed), the structure of the (113) defects and the parameters of the related luminescence centers are not changed. To our knowledge, we were the first to study the temperature dependence of the intensity of the EL line associated with (113) defects. A significant difference from the PL data is that there is no portion at which a buildup of the EL intensity is observed with increasing current density at low temperatures [12, 13].

The experimental values (points) of the half width of the EL line of (113) defects (full width at half-maximum, FWHM) are shown at different temperatures in Fig. 4 for a current density of 4.61 A/cm^2. With increasing temperature, the FWHM grows. The experimentally determined temperature dependence of the FWHM (in nm) is well approximated, as also in the case of PL, by a linear dependence (solid line in Fig. 4)

$$\mathrm{FWHM} = aT + b, \quad (4)$$

where $a = 0.143$ nm/K and $b = 22.2$ nm. In the case of EL, the FWHM of the line associated with (113) defects increases as compared with the PL: the slopes of the

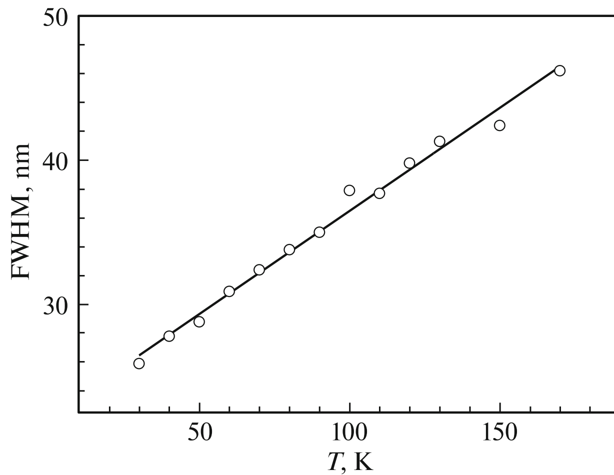

Fig. 4. Temperature dependence of the FWHM of the luminescence line associated with (113) defects and its approximation with formula (4) (solid line).

straight lines (constant a) nearly coincide for both kinds of luminescence excitation, and the value of constant b becomes 1.7 times larger [12]. Previously, the broadening of luminescence lines with increasing measurement temperature has been observed for lines $D1$ and $D2$ of dislocation-related luminescence and those formed with the involvement of intrinsic interstitial silicon atoms [17].

4. CONCLUSIONS

LED structures with luminescence from (113) defects were fabricated for the first time. p–n junctions were produced by the diffusion of boron, and (113) defects were formed in the course of the implantation of oxygen ions and subsequent annealing. The dependences of the main parameters of the EL line on the measurement temperature and pump-current density were examined. The peak energy (in eV) of the line associated with the (113) defect shifts with increasing temperature to longer wavelengths in parallel with the decrease in the band-gap width, being described by the formula $E_{113} = 907 - 0.49T^2/(T + 655)$. As the temperature increases to ~70 K, the intensity of the EL line grows at low current densities (<2.59 A/cm^2) with a buildup activation energy of 25 meV and at higher densities it is temperature independent. With increasing measurement temperature, the intensity decreases with a quenching activation energy of 59 meV, and the line is still recorded at 170 K. The full width of the line at half-maximum linearly grows with increasing temperature: FWHM = $0.143T + 22.2$. A broadening of the EL line as compared with the photoluminescence line was observed. Using defect-engineering methods suggests that light-emitting diode structures with room-temperature EL from the (113) defect at a wavelength of ~1370 nm will be created in the near future.

CONFLICT OF INTEREST

The authors state that they have no conflict of interest.

REFERENCES

1. G. Franzo, F. Priolo, S. Coffa, A. Polman, and A. Carnera, Appl. Phys. Lett. **64**, 2235 (1994).
2. N. A. Sobolev, A. M. Emel'yanov, and K. F. Shtel'makh, Appl. Phys. Lett. **71**, 1930 (1997).
3. V. Kveder, V. Badylevich, W. Schröter, M. Seibt, E. Steinman, and A. Izotov, Phys. Status Solidi A **202**, 901 (2005).
4. N. A. Sobolev, A. E. Kalyadin, M. V. Konovalov, P. N. Aruev, V. V. Zabrodskiy, E. I. Shek, K. F. Shtel'makh, A. N. Mikhaylov, and D. I. Tetel'baum, Semiconductors **50**, 240 (2016).
5. S. Takeda, Jpn. J. Appl. Phys. **30**, L639 (1991).
6. L. I. Fedina, A. K. Gutakovskii, A. V. Latyshev, and A. L. Aseev, in *Advances in Semiconductor Nanostructures, Growth, Characterization, Properties and Applications*, Ed. by A. Latyshev, A. Dvurechenskii, and A. Aseev (Elsevier, Amsterdam, 2016), p. 383.
7. L. Jeyanathan, E. C. Lightowlers, V. Higgs, and G. Davies, Mater. Sci. Forum **143–147**, 499 (1994).
8. S. Coffa, S. Libertino, and C. Spinella, Appl. Phys. Lett. **76**, 321 (2000).
9. D. C. Schmidt, B. G. Svensson, M. Seibt, C. Jagadish, and G. Davies, J. Appl. Phys. **88**, 2309 (2000).
10. Y. Yang, J. Bao, C. Wang, and M. J. Aziz, J. Appl. Phys. **107**, 123109 (2010).
11. N. A. Sobolev, A. E. Kalyadin, P. N. Aruev, V. V. Zabrodskii, E. I. Shek, K. F. Shtel'makh, and K. V. Karabeshkin, Phys. Solid State **58**, 2499 (2016).
12. N. A. Sobolev, A. E. Kalyadin, E. I. Shek, and K. F. Shtel'makh, Semiconductors **51**, 1133 (2017).
13. N. A. Sobolev, A. E. Kalyadin, E. I. Shek, K. F. Shtel'makh, V. I. Vdovin, A. K. Gutakovskii, and L. I. Fedina, Phys. Status Solidi A **214**, 1700317 (2017).
14. J. F. Ziegler, M. D. Ziegler, and J. P. Biersack, Nucl. Instrum. Methods Phys. Res., Sect. B **268**, 1818 (2010).
15. V. Alex, S. Finkbeiner, and J. Weber, J. Appl. Phys. **79**, 6943 (1996).
16. S. Binetti, S. Pizzini, E. Leoni, R. Somaschini, A. Castaldini, and A. Cavallini, J. Appl. Phys. **92**, 2437 (2002).
17. N. A. Sobolev, Semiconductors **44**, 1 (2010).
18. L. Xiang, D. Li, L. Jin, S. Wang, and D. Yang, J. Appl. Phys. **113**, 033518 (2013).
19. G. Davies, Phys. Rep. **176**, 83 (1989).

Translated by M. Tagirdzhanov